A Quantitative Structure-Activity Relationship Analysis of Some 4-Aminodiphenyl Sulfone Antibacterial Agents Using Linear Free Energy and Molecular Modeling Methods

Rosa L. Lopez de Compadre,† R. A. Pearlstein,† A. J. Hopfinger,*† and J. K. Seydel‡

Department of Medicinal Chemistry and Pharmacognosy, University of Illinois at Chicago, Chicago, Illinois 60680, and Borstel Research Institute, Institute for Experimental Biology and Medicine, D-2061 Borstel, Federal Republic of Germany.
Received July 24, 1986

A set of 36 congeneric 4-aminodiphenyl sulfones with measured inhibition potencies of dihydropteroate synthase were studied by using both linear free energy and molecular modeling methods. The goals of the investigation were to identify the "active" conformation for these compounds as inhibitors and, correspondingly, to construct a quantitative structure–activity relationship (QSAR). These molecules are quite flexible and possess multiple conformational energy minima. Application of molecular shape analysis (MSA), using all intramolecular energy minima as part of the analysis, was not successful in generating a QSAR. However, the calculated intramolecular conformational entropy of these compounds was found to correlate with inhibition potency leading to a highly significant QSAR. Inhibition potency increases as entropy decreases. A decrease in entropy enhances the population of specific, symmetry-related minimum-energy conformations. In this indirect way, it was possible to postulate an "active" conformation. This investigation illustrates that specific knowledge of the "active" shape of a molecule may not provide the information needed to quantitatively explain the observed structure–activity relationship.

Although of limited utility in the management of many bacterial infections, 4,4′-diaminodiphenyl sulfone (dapsone, DDS, I) is a uniquely effective bacteriostatic agent against acid-fast bacteria and especially *Mycobacterium leprae*.

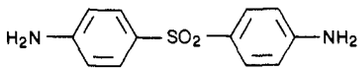

I

While dapsone has remained the agent of choice, used singly or in combination, in the chemotherapy of leprosy for a number of years, few definitive investigations of its mechanism of action, of its structure–activity relationships, or of the reasons underlying the development of dapsone resistance have been reported. This is principally due to the lack of in vitro models since the *M. leprae* organism remains virtually impossible to grow in cultures.

Recently a mycobacterial strain called *M. lufu* has been examined by Seydel and co-workers[1] and found to be similar to *M. laprae* in many respects including some growth conditions, kinetics, and sensitivity to various antimycobacterial agents, especially to dapsone.

The dihydropteroate synthase inhibitory activities of a series of 4-aminodiphenyl sulfone derivatives (II), dapsone analogues, in a cell-free folate synthesizing enzyme extract from *M. lufu*, were determined by Seydel and co-workers.

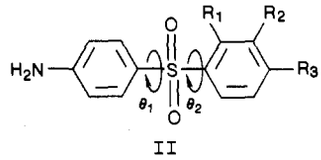

II

Inhibition studies were conducted by determination of the extract folate production at standardized incubation times in the presence of 8–10 varying concentrations of inhibitor. *M. lufu* extracts were incubated for 8 h at 31 °C. All components were present in the same concentrations with the exception of added inhibitor.

The rate of folate production with respect to time was determined by periodic sampling of the incubation mixtures and quenching the reaction by addition of trichloroacetic acid. Amounts of folate produced were determined with folate-requiring *Streptococcus faecium*. That is, the amount of dihydropteroic acid synthesized by the enzyme was measured microbiologically with *Streptococcus* strains that need the pteroic acid to grow. Fifty percent inhibitory concentrations (I_{50}) were calculated by using a curve-fitting procedure. Inhibition experiments were repeated until the computed 95% confidence interval for the I_{50} value fell within ±15%. The I_{50} values in micromoles/liter were transformed to pC units (log $1/I_{50}$) and are reported as part of Table I.

Analyses of the structure–activity data on these compounds, using multiple regression and principal component methods, indicated that quantitative structure–activity relationships (QSARs) could be constructed for subsets of the total data base.[1] These QSARs involved measured differences in NMR shifts as correlation descriptors to inhibition potency. Differences in chemical shifts are sensitive measures of electron withdrawal or donation. Thus, Seydel and co-workers concluded that the electronic influence of the substituents R_1, R_2, and/or R_3 is responsible for inhibition potency.[1]

Still, it was annoying that no single "universal" QSAR could be formulated to explain the variation in inhibition potency for the entire set of compounds reported in Table I. Seydel suggested to us that this structure–activity data base might be an interesting challenge for the methods and strategies devised in our laboratory to generate QSARs based upon both linear free energy and/or group additive descriptors, as well as those realized from three-dimensional molecular modeling.[2] The goal of the work reported below was to identify a universal QSAR for the compounds in Table I.

Methods

A. Model Building. The aromatic rings and substituents to these rings were constructed with standard bond lengths and bond angles.[3] The bond lengths and angles for the $-SO_2-$ group were taken from a composite analysis of the structures of some simple compounds.[4] An initial

† University of Illinois at Chicago.
‡ Borstel Research Institute.

(1) Coats, E. A.; Cordes, H.-P.; Kulkarni, V. M.; Richter, M.; Schaper, K.-J.; Wiese, M.; Seydel, J. K. *J. Quant. Struct.-Act. Relat.* **1985**, *4*, 99.
(2) Mabilia, M.; Pearlstein, R. A.; Hopfinger, A. J. *Eur. J. Med. Chem.* **1985**, *20*, 163 and references therein.
(3) Hopfinger, A. J. *Conformational Properties of Macromolecules*; Academic: New York, 1973.
(4) *Handbook of Chemistry and Physics*, CRC: Boca Raton, FL, 1985.

0022-2623/87/1830-0900$01.50/0

Table I. Structure–Activity Data on the 4-Aminodiphenyl Sulfone Dihydropteroate Synthase Inhibitors

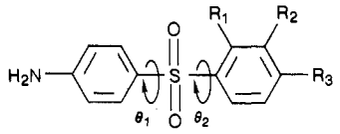

no.	R_1	R_2	R_3	pC obsd	pC pred	Δ (obsd − pred)	S, cal/(mol·K)	$(\theta_1, \theta_2) = (0°, 60°)$ minimum present[a]
1	Cl	H	NH_2	6.32	6.25	0.07	5.34	Y
2	CH_3	H	NH_2	6.19	6.23	−0.04	9.22	Y
3	OH	H	NHC_2H_5	6.14	6.18	−0.04	14.70	Y
4	H	OH	NH_2	6.07	6.14	−0.07	21.29	N
5	H	H	$NHCH_2COOH$	6.06	6.09	−0.03	27.87	Y
6	OCH_3	H	NHC_4H_9	5.99	6.05	−0.06	33.01	N
7	NH_2	H	NH_2	5.99	6.02	−0.03	36.66	Y
8	OCH_3	H	NHC_3H_7	5.92	6.01	−0.09	37.92	N
9	H	H	NH_2	5.92	5.96	−0.04	44.59	Y
10	NO_2	H	NH_2	5.87	5.94	−0.07	47.20	Y
11	H	H	$NHCH_3$	5.89	5.89	0.00	53.84	Y
12	H	H	OH	5.82	5.84	−0.02	60.51	Y
13	OCH_3	H	NHC_2H_5	5.75	5.84	−0.09	60.69	N
14	H	H	$N(CH_3)_2$	5.75	5.79	−0.04	67.34	Y
15	OCH_3	H	NH_2	5.73	5.75	−0.02	72.23	N
16	H	OH	NHC_2H_5	5.70	5.71	0.02	78.83	N
17	OH	H	NHC_3H_7	5.71	5.66	0.05	84.38	Y
18	H	OH	NHC_3H_7	5.64	5.61	0.03	91.00	N
19	H	H	$NHCH_2COOCH_3$	5.65	5.56	0.09	97.60	Y
20	CN	H	NH_2	5.65	5.54	0.11	100.2	Y
21	H	OCH_3	NH_2	5.56	5.50	0.06	106.5	Y
22	NH_2	H	H	5.65	5.47	0.18	110.3	Y
23	H	H	NHC_2H_5	5.56	5.42	0.14	116.9	Y
24	H	OCH_3	NHC_2H_5	5.49	5.37	0.12	123.2	Y
25	NO_2	H	H	5.61	5.35	0.16	126.3	Y
26	H	H	COOH	5.44	5.30	0.14	133.0	Y
27	H	OCH_3	NHC_3H_7	5.40	5.26	0.14	139.0	Y
28	H	H	$NHCOCH_3$	5.15	5.21	−0.06	145.6	Y
29	H	H	OCH_3	5.12	5.11	0.01	152.3	Y
30	H	H	CH_3	5.09	5.11	−0.02	158.9	Y
31	NH_2	H	NO_2	4.93	5.08	−0.15	162.1	Y
32	H	H	$COOCH_3$	4.93	5.03	−0.10	168.7	Y
33	H	H	H	4.92	4.98	−0.06	175.5	Y
34	H	H	$CONHNH_2$	4.90	4.93	−0.03	182.1	Y
35	H	H	Cl	4.89	4.88	0.01	188.8	Y
36	H	H	NO_2	4.51	4.83	−0.32	195.4	Y

[a] Y = yes, N = no.

fixed-valence geometry conformational search[5] at 30° increments about θ_1 and θ_2, as defined in II, was made with a dispersion–steric repulsion energy term. The potential set developed by Hopfinger was employed[3] for each compound in the data base. Torsional rotations at 30° increments were also done about bonds in flexible substituents. The lowest energy conformer identified in each of the conformational scans was selected as the sterically acceptable conformer to use in the calculation of the charge density distribution.[6] The CNDO/2 method was used to compute the charge densities.[7]

Each compound was next subjected to a free valence geometry (total) energy minimization[8] with the minimum-energy conformers identified in the initial steric scans as the minimization starting points. Force constants and torsional parameters for the $-SO_2-$ group were determined by using the MINDO/3 semiempirical molecular orbital method[9] and the fixed valence geometry molecular mechanics force field suggested by Hopfinger.[3] The strategy to compute force constants and torsional barriers given in ref 6 was employed. The other force constants and torsional parameters were available. The resulting valence geometries determined in each of these complete structure optimizations were held constant in all subsequent conformational searches.

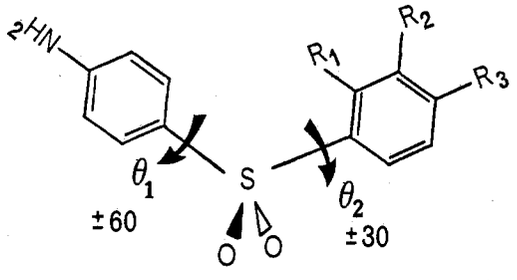

Figure 1. The reference conformation of the aminodiphenyl sulfones for which $\theta_1 = \theta_2 = 0°$. The ±60° and ±30° denote the set of rotations that give rise to the four possible active conformations.

B. Conformational Analysis. Uniform scanning at 30° increments was carried out for θ_1 and θ_2 (see II) and

(5) Orchard, B. J.; Tripathy, S. K.; Pearlstein, R. A.; Hopfinger, A. J. *J. Comput. Chem.* **1987**, *8*, 28.
(6) Hopfinger, A. J.; Pearlstein, R. A. *J. Comput. Chem.* **1984**, *5*, 486.
(7) Pople, J. A.; Beveridge, D. C. *Approximate Molecular Orbital Theory*; McGraw-Hill: New York, 1970.
(8) The MMFF option of the CHEMLAB-II molecular modeling system was used. This is a modified Allinger Force Field; Allinger, N. L. *J. Am. Chem. Soc.* **1977**, *99*, 8127.
(9) Bingham, R. C.; Dewar, M. J. S.; Lo, D. H. *J. Am. Chem. Soc.* **1975**, *97*, 1302.

for torsional rotations in flexible substituents R_1, R_2, and/or R_3. The fixed valence geometry force field defined in the model building phase of the analysis was used to evaluate the intramolecular energetics. The relative $\theta_1 = \theta_2 = 0°$ conformer, defined as the reference conformation in these analyses, is that shown in Figure 1. Both aromatic rings are coplanar in this reference conformation with R_1 pseudotrans to the SO_2 oxygens with respect to θ_2.

Conformational scans were carried out for each of the compounds reported in Table I. Corresponding conformational energy maps for θ_1 and θ_2 were constructed for each compound. In order to characterize and compare the conformational profiles of these compounds, the energy maps were divided into quadrants as defined by lines through $\theta_1 = 180°$ and $\theta_2 = 180°$. The minimum energy conformer states of flexible substituents were determined as a function of their torsional rotations for each choice in θ_1 and θ_2 as part of the conformational scan involving θ_1 and θ_2.

C. QSAR Descriptors. Linear free energy and/or group additive as well as three-dimensional molecular modeling features were generated as possible correlation descriptors to antibacterial potency. These descriptors included the following.

1. log P of the entire molecule and π_{R_1}, π_{R_2}, π_{R_3}, and combinations of $(\pi_{R_i} + \pi_{R_j})$ for the substituents R_1, R_2, and R_3.[10] These lipophilicity descriptors were determined by using the Leo and Hansch method.[11]

2. Hammett's electron-withdrawing indice σ for the three possible substituents.[12]

3. Common overlap steric volume between pairs of superimposed molecules set in specific conformer states with molecular shape analysis (MSA).[2] The selected conformer states were chosen from the set of calculated intramolecular minima. Each minimum-energy conformer served as a shape reference to which all other compounds were compared. Two criteria for molecular superposition were considered: The two common 4-aminophenyl aromatic rings from each compound were placed in common and, secondly, the SO_2 groups were placed over one another.

4. The free space intramolecular conformational entropy[3] as measured by

$$S = -R \sum_{i=1}^{N} P_i \ln P_i \qquad (1)$$

where R is the gas constant, N the number of conformational states sampled, and P_i is the Boltzmann probability of the ith conformational state. The P_i, in turn, were computed from the fundamental statistical mechanics relationship[13]

$$P_i = \frac{\exp(-E_i/RT)}{\sum_{i=1}^{N} \exp(-E_i/RT)} \qquad (2)$$

where E_i is the intramolecular conformational energy of the ith state.

5. The absolute conformational energy of the global minimum energy conformer state.

6. Differences in conformational energy between pairs of intramolecular minima of a given compound. The idea in using energy differences between stable conformational states of a compound is that one conformer might be the critical "active" conformation. The energy difference between this state and some other conformer would then be an activation energy for biopotency. Along the same lines, the energy required to "move" a compound into the active conformation might also be considered an activation energy. We adopted this concept and applied ti to each of the minimum-energy conformers of the active compounds, which are not minima for inactive compounds, as candidates for the "active" conformation. The maximum barrier energy needed to move from the "closet" local minimum, based on bond rotations, to each of these "active" states was computed as a potential QSAR descriptor.

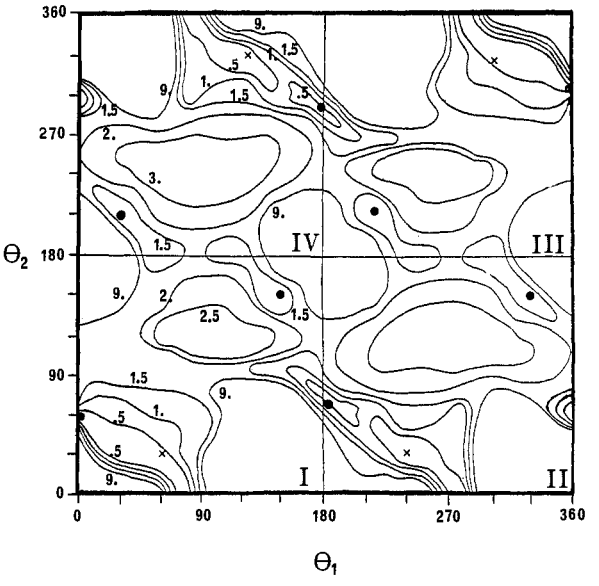

Figure 2. Conformational energy map of θ_1 vs. θ_2 for the active inhibitor (R_1 = Cl, R_2 = H, R_3 = NH_2), compound 1 of Table I. Energy contours are in kilocalories/mole above the global energy minimum denoted by X. Relative energy minima are denoted by heavy dots. The map is divided into quadrants; see text.

D. Statistical Analysis. The multivariational matrix containing inhibitory potency and molecular descriptors as columns and compounds as rows was preanalyzed by using two blocks partial least squares principal component analysis CPLS2.[14] A program to perform this analysis is part of SIMCA, a statistical software package for pattern recognition studies.[15] Combinatorial descriptor set multiple linear regression analysis was subsequently performed, with SIMCA, to compute QSARs. No more than three descriptors were used at a time as independent variables in performing a multiple linear regression analysis.

Results

Conformational analyses of 36 4-aminodiphenyl sulfones indicate that these molecules are quite flexible with respect to θ_1 and θ_2. The compounds studied are listed in Table I. Ortho substitution (R_1) diminishes conformational flexibility, as compared to meta and/or para substituents. Nevertheless, even the ortho-substituted compounds exhibit multiple intramolecular minima and significant conformational freedom. Conformational energy maps for the highly active analogue, compound 1 of Table I (R_1 = Cl, R_2 = H, R_3 = NH_2), and an inactive congener, compound 35 of Table I (R_1 = H, R_2 = H, R_3 = Cl), are shown

(10) Hansch, C.; Clayton, J. M. *J. Pharm. Sci.* **1973**, *62*, 1.
(11) Hansch, C.; Leo, A. *Substituent Constants for Correlation Analysis in Chemistry and Biology*; Wiley-Interscience: New York, 1979.
(12) Charton, M. CHEMTECH **1974**, No. 502.
(13) Flory, P. J. *Statistical Mechanics of Chain Molecules*; Wiley-Interscience: New York, 1969.
(14) Wold, S.; Hellber, S.; Dunn, W. J., III *Acta Pharmacol. Toxicol.* **1983**, *52*, 158.
(15) Dunn, W. J., III; Wold, S. *Bioorg. Chem.* **1980**, *9*, 505.

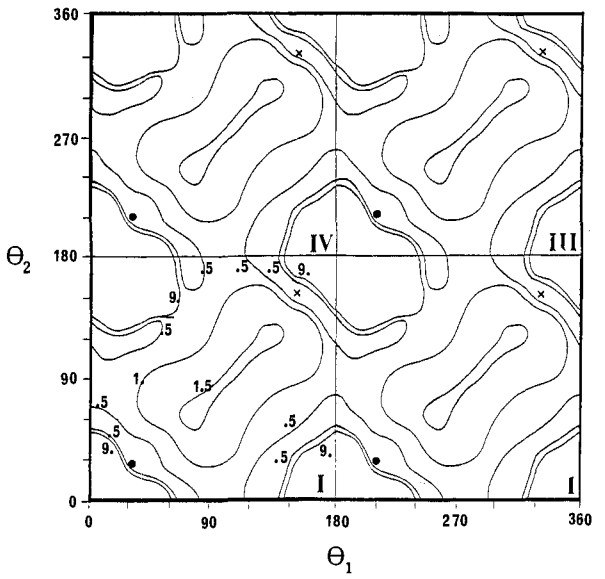

Figure 3. Same as Figure 1 but for the inactive inhibitor (R_1 = H, R_2 = H, R_3 = Cl), compound **35** of Table I.

in Figures 2 and 3, respectively. These energy maps are representative of compounds in this series having ortho substituents (Figure 2) or only meta and/or para substituents (Figure 3). The inactive analogue has eight intramolecular energy minima. The energy map of the inactive analogue can also be divided into four symmetric quadrants by constructing lines through $\theta_1 = 180°$ and $\theta_2 = 180°$. Isoenergy contour values are only given in quadrant I because of the symmetry. Each quadrant contains two minimum-energy conformers that are symmetry related to one another and all other minima by rotations about θ_1 and/or θ_2 from the reference conformation in which the aromatic rings are coplanar as shown in Figure 1.

Ortho substitution of the chlorine in the active analogue introduces asymmetry into the conformational profile. The corresponding energy map (Figure 2) has four minima in common with minima of the inactive congener. These four conformations were eliminated as possible candidates for the "active" conformation of this class of compounds on the assumption that active compounds possess a distinct conformation not readily accessible to inactive analogues. The other four minima observed in the inactive compound each "split" into a pair of new minimum-energy conformers in the active compound. Further, the symmetry of the four quadrants is partially lost in the energy map of the active analogue. Quadrants 1 and 3 and quadrants 2 and 4 (see Figure 2) are, respectively, symmetric. Isoenergy contour values are only given for quadrants I and IV because of the symmetry of the energy surface. These changes in the conformational behavior of the active compound, as compared to the inactive analogue, arise largely because of interaction between the ortho chlorine and the SO_2 group. Table II summarizes location of intramolecular minima in active and inactive analogues.

The four pairs of split minima observed for compound 1 of Table I contain four minimum energy conformer states realized among both the active and inactive analogues reported in Table I. These minima are (θ_1, θ_2) = (0°, 60°)/(180°, 60°)/(360°, 300°)/(180°, 300°). Table I lists the presence, or absence, of these minima with the (0°, 60°) conformer as a representative member of this set. The remaining four symmetry-related minima, (θ_1, θ_2) = (60°, 30°)/(240°, 30°)/(300°, 330°)/(120°, 330°), are only present in the active analogues and, thus, were considered

Table II. Intramolecular Energy Minima of an Active (Compound 1 of Table I) and an Inactive (Compound **35** of Table I) 4-Aminodiphenyl Sulfone Antibacterial Agent

active compounds			
θ_1,[a] deg	θ_2,[a] deg	quadrant[b]	energy,[c] kcal/mol
0	60	1	0.2
60	30	1	0.1
150	150	1	1.3
180	60	2	0.2
240	30	2	0.0
330	150	2	1.5
360	300	3	0.2
300	330	3	0.1
210	210	3	1.3
180	300	4	0.2
120	330	4	0.0
30	210	4	1.5
30	30	1	0.0
150	150	1	0.2
210	30	2	0.0
330	150	2	0.2
210	210	3	0.0
330	330	3	0.2
30	210	4	0.0
150	330	4	0.2

[a] The reference conformation, $\theta_1 = \theta_2 = 0°$, has the two aromatic rings coplanar. [b] The quadrants are defined in the energy maps shown in Figures 2 and 3. [c] This energy is relative to the global energy minimum for which $E = 0.0$ kcal/mol.

as "active" conformation candidates. These conformer states, using the (60°, 30°) conformation as a representative, were consequently used in the MSA. However, it was not possible to establish any significant correlation between the common overlap steric volume between pairs of superimposed molecules, which is an established descriptor for shape similarity/difference,[2] and inhibition potency using the postulated "active" conformation, (θ_1, θ_2) = (60°, 30°), as the shape reference state. By symmetry this finding would be identical if any of the three other possible "active" conformers had been used as the reference conformation.

An alternate strategy to identifying critical conformational states was undertaken on the basis of conformational energetics. One approach was to compute the sets of energies required to move a compound from each of the minimum energy conformer states common to both active and inactive analogues to the corresponding split minima conformations accessible only to the active analogues. Here, as in the MSA investigation, the linear free energy and group additive descriptors described in the methods section were used in combination (in this case) with differences in conformational energies to establish possible correlations with inhibition potency. Again, no QSAR could be established.

A second set of conformational "activation" energies were considered on the basis of the observation that four of the minimum-energy conformations common to active and inactive inhibitors, (θ_1, θ_2) = (150°, 150°)/(330°, 150°)/(210°, 210°)/(30°, 210°), become higher in energy, relative to the postulated "active" conformer minima, as inhibitor potency increases. Thus, conformational energy differences between pairs of members of these two conformer sets located in the same quadrant of the energy map were computed and used as activity descriptors. No significant QSAR was found.

The absolute conformational energies of the minima of active analogues tend to be lower (more stable) than the minimum energies of the less active analogues. This can be seen in Figure 4 where the absolute calculated conformational energies of a highly active, a moderately active,

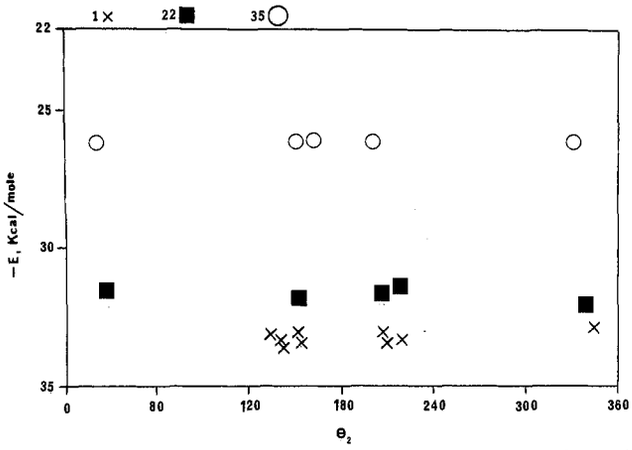

Figure 4. The absolute conformational energy in kilocalories/mole for a highly active compound (1), a moderately active analogue (**22**), and an inactive diphenyl sulfone (**35**) as a function of θ_2.

and an inactive compound are plotted as a function of θ_2 (with the energy minimized with respect to the other degrees of freedom). Unfortunately, no set of absolute conformational energies of any of the stable conformers could quantitatively be related to inhibition potency.

An analysis of the θ_1 vs. θ_2 conformational energy maps indicates that active compounds are more rigid than inactive analogues. Further, the conformational states at, and around, the split pairs of minima (see Figures 2 and 3 as examples) constitute the great majority of populated states in active analogues. We opted to compute the intramolecular conformational entropy, S, using eq 1 and 2 arising from all torsional rotations, and to use S as a QSAR descriptor. A highly significant QSAR was established in which S is simply a linear correlate to inhibition potency:

$$pC = 6.30 - 0.0075\ (\pm 0.0006)S \qquad (3)$$

$$N = 36,\ R = 0.970,\ \mathrm{SD} = 0.11,\ F = 544.6$$

Equation 3 accounts for over 93% of the variance in the inhibition measurements reported in Table I. This QSAR may be too good in that the standard deviation of fit might be less than the uncertainty in the experimental measurement. This does not turn out to be the case. The standard deviation in experimental measurement is ±0.06.

It is difficult to understand why intramolecular conformational entropy is a key correlation descriptor to bioactivity if one thinks in terms of a direct lock and key fit between the ligand and the receptor. Equation 3 does, however, indirectly support the "active" conformation hypothesis involving four of the split minima of which (θ_1, θ_2) = (60°, 30°) is a representative member. The QSAR indicates that, as entropy decreases, inhibition potency increases. A decrease in entropy, however, is realized by an increase in the population of the four pairs of split minima shown in Figure 2. Thus, the hypothesized "active" conformations, of which (θ_1, θ_2) = (60°, 30°) is a representative member, become more populated as activity increases. Unfortunately, it is not possible to pick which of the four minima is the active conformation. These four "active" conformation candidates are, as noted earlier, symmetry related. Each can be generated by a θ_1 rotation of ±60° and a θ_2 rotation of ±30° from the reference conformation. Figure 5 shows stereomolecular models of the active analogue (R_1 = Cl, R_2 = H, R_3 = NH_2), compound 1 in Table I, in one of the postulated active conformations, (θ_1, θ_2) = (60°, 30°).

Seydel et al.[1] determined the chemical shifts of the 4-amino protons and the 2,6-aromatic ring protons in 1% solutions of Me_2SO-d_6 at room temperature. The change in chemical shift as a function of R_1, R_2, and/or R_3, Δppm, was determined relative to the 4-H congener. These workers also determined the fraction of ionization, f_i, for ionizable groups in the 4-position. The values of f_i were measured at pH 7.75, which corresponds to experimental conditions.

These two experimental descriptors combined with the calculated value of molecular refractivity of R_2, MR_2, also yield a QSAR for the structure–activity data given in Table I for the 4-aminodiphenyl sulfones:

$$pC = -5.91\Delta\mathrm{ppm} + 0.507f_i + 0.047MR_2 = 5.06 \qquad (4)$$

$$N = 36,\ R = 0.90,\ S = 0.19,\ F = 47.56$$

Equation 4 is similar in form to QSARs established by Seydel and co-workers[1] on other similar structure–activity data bases.

A correlation relationship can be established between the descriptors in eq 4 and S:

$$S = 776\Delta\mathrm{ppm} - 59.8f_i - 6.1MR_2 + 167.8 \qquad (5)$$

$$N = 36,\ R = 0.91,\ S = 0.24,\ F = 52.2$$

Equation 5 suggests that the free space intramolecular entropy should decrease as the compound becomes ionized and as the value of MR_2 increases. Both of these relationships make intuitive sense. The electrostatic interactions involving an ionized group place greater conformational restrictions on a molecule as compared to interactions involving the neutral form of the group. Thus, entropy should decrease. MR_2 is, in part, a measure of the size of R_2. As the size of R_2 increases, conformational flexibility, with respect to θ_1 and θ_2, decreases as can be seen in Figure 3. A loss in flexibility of torsional rotation again coresonds to a decrease in entropy.

The direct dependence of S on Δppm is not clear. This relationship may, in part, be due to the way in which Δppm is defined (relative to the chemical shift of the 4-H congener).

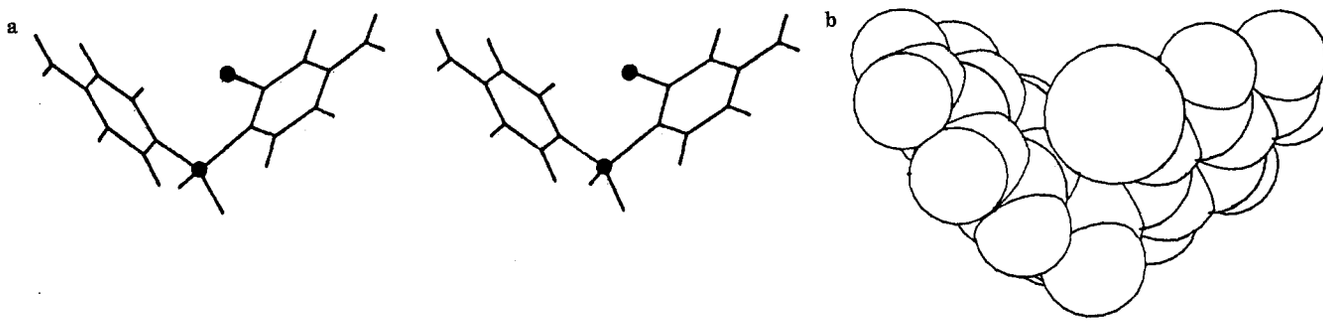

Figure 5. (a) Stereo stick and (b) space-filling representations of the "active" conformation for compound 1 of Table I, θ_1 = 60°, θ_2 = 30°.

Overall, eq 5 establishes a physically reasonable relationship between the descriptors of two distinct QSARs, both of which account for the observed variability in biopotency of a common set of compounds.

Discussion

The key finding in this study is that the calculated intramolecular conformational entropy of the substituted 4-aminodiphenyl sulfones quantitatively correlates with inhibition potency against dihydropteroate synthase. As the entropy decreases, inhibition potency increases. It is difficult to speculate a mechanism of action of the 4-aminodiphenyl sulfones that is consistent the QSAR. Perhaps the inactive, higher entropy analogues cannot find the correct enzyme-binding conformation quick enough after initial contact with the enzyme so that the complex breaks up before tighter binding can occur. This model of enzyme inhibition would be characterized as follows: There is a weak initial binding of the ligand to the enzyme. The ligand can be in any sterically acceptable conformer state. Once weakly bound, the ligand undergoes a conformational relaxation. This relaxation process ultimately leads to a particular conformational state (the "active" conformation) that enhances binding. At the same time, however, conformational fluctuations in both the ligand and enzyme during the relaxation process can lead to the destruction of the initial binding.

This model is consistent with the QSAR in that a decrease in conformational entropy should decrease the time needed to find the stronger binding conformation and, thereby, increase inhibition potency. The ligand conformational fluctuations should also be less in rigid (low entropy) analogues, thus decreasing the probability of breaking up the complex. Such behavior should also contribute to increased inhibition potency. The model also explains why molecular shape descriptors do not correlate well with biopotency even though an "active" conformation can be projected from the QSAR. The loss in conformational entropy in active analogues enhances the population of the four split pairs of conformations. One of these conformations is postulated to be the "active" conformation. However, the model identifies the time needed to realize this conformation upon weak binding, as indirectly measured by conformational entropy, as the key factor controlling inhibition potency.

This QSAR and postulated model of enzyme inhibition have a profound implication on molecular modeling in drug design. An implicit working assumption in most molecular modeling studies is that a particular conformation and/or shape of a compound is responsible for its bioactivity. Identification of the active conformation/shape is considered the major piece of information needed to do molecular design. The work reported here indicates this may not always be the case even when an active conformation can be identified. Rather, properties related to conformation, but not even expressed in terms of spatial measurements, may have to be evaluated as possible key descriptors that *quantitatively* account for the variation in biological potency.

Avbdelj and Hazdi[16] have reported that conformational entropy is related to biological activity in a set of clonidine analogues. These workers have computed the entropy in the same manner as done in this work (eq 1 and 2). However, their method of computing the conformational energetics, required for computing entropy, differs from our approach in both force field and parameters, as well as the procedural methods for exploring conformational space.

The QSARs given by eq 3 and 4 represent two independent representations of a common structure–activity data base. One QSAR is based totally on computation (eq 3) and the other largely on experimental measurements. Nevertheless, it is significant that the relationship established between the independent variables, S in eq 3, and Δppm, f_i, and MR_2 in eq 4, as given by eq 5, makes intuitive sense. In this regard the two QSARs mutually support one another. A quantitative example of this mutual support, which leads to a successful prediction, involves the 4-Br analogue. This compound was made and tested after eq 3 was derived from the data in Table I. The value of S for the 4-Br analogue was estimated to be 166 from eq 5. This leads to a predicted pC value of 5.05. The observed value is 4.92. The calculated value of S for 4-Br using conformational analysis is 191, which predicts pC = 4.87.

Free-space intramolecular conformational entropy is a more significant correlation descriptor to pC than the combination of Δppm MR_2, and f_i as judged by the measures of statistical fit. This, in turn, suggests that S more closely reflects/measures the causative factors for variance in inhibition potency.

Lastly, some comments on the absolute calculated conformational energies and entropies are in order. The more active compounds tend to have lower absolute minimum energies than inactive analogues. Generally, absolute stabilization energy for neutral molecules (neglecting hydrogen bonding) increases as the number of atoms increases since the number of attractive dispersion interactions is a direct function of the number of atoms. Usually, electrostatic interactions do not play a major role in absolute energetics, but can be critical to entropy. Thus, one might expect the larger (in terms of R_1, R_2, and R_3) 4-aminodiphenyl sulfones to be the more active compounds. Even a cursory analysis of Table I indicates that molecular size (number of atoms) does not correlate with activity. In this particular class of compounds, the lower absolute conformational energy in the more active analogues appears to be a result of the active molecule fitting together better (lower entropy) with respect to both steric contacts and electrostatic interactions, which includes weak hydrogen bonding. Thus, the finding of a partial relationship between absolute conformational energy and pC is an example of "parameter aliasing". That is, absolute conformational energy is a partial stand-in for S.

The increase in conformational entropy in the inactive analogues does not arise from any single class of energy terms. Rather dispersion, electrostatic, hydrogen-bonding, and torsional contributions each make dominant contributions to specific compounds over the data base to produce the calculated entropic behavior. For example, compounds **6**, **8**, **13**, and **15** of Table I successively differ from one another by deletion of a methylene unit in the para substituent with increasing compund number and corresponding loss in inhibition potency. Generally, deletion of methylene spacers should decrease the flexibility of the substituent and thereby decrease the intramolecular entropy. The opposite is found in compounds **6**, **8**, **13**, and **15** because the larger flexible para substituents, according to our *free-space* intramolecular conformational analyses, fold back over the rest of the molecule due to favorable dispersion interactions. These highly preferred folded states deplete the total entropy of the compound. The greater the number of methylene spacers, the more tightly

(16) Abvdelj, F.; Hazdi D. In *QSAR and Strategies in the Design of Bioactive Compounds*; Seydel, J. K., Ed.; VCH Verlagsgesellschaft: Berlin, Fed. Rep. Ger., 1985; p 83.

folded is the molecule and the lower its entropy.

Equation 3 is based upon the free-space intramolecular conformational entropy. If the effects of solvent are included in the estimation of S, the relationship between pC and S partly breaks down. In essence, the highly folded, energetically preferred conformations found in free space for flexible substituents, lose their energetic preference in a simulated solvent medium, and the entropy increases. This was observed when the aqueous hydration shell model[3] was used to take into account solvation energetics as part of the conformational analysis.

It is difficult to speculate why the entropy associated with free-space conformational behavior best correlates with inhibition potency. Perhaps the shape of the receptor site limits the conformational behavior of the substituents upon initial binding and keeps them restricted throughout the binding process.

The role of electrostatic and hydrogen-bonding interactions on intramolecular entropy can be realized by comparing compounds **4** and **21** of Table I. These compounds differ by R_2 = OH for 4 vs. R_2 = OCH_3 for **21**. The lower entropy of compound **4** is a result of combined electrostatic–hydrogen bond interaction between the hydroxyl and the SO_2 oxygens. This stabilizing set of interactions, which are not possible for the methoxy group of compound **21**, limits conformational flexibility and, consequently, lowers entropy relative to compound **21**.

The examples cited above illustrate that molecular modeling can sometimes lead to results that are different from our intuitive feelings. At the same time, modeling calculations can be dissected to identify the reasons why the calculations are not consistent with intuition. In so far as the reasons found in the calculations are valid, molecular modeling may offer us an unbiased, new way of looking at some of our structure–activity problems.

Acknowledgment. We very much appreciate the assistance of Professor W. J. Dunn III (UIC) during the course of this investigation and Dr. C. Compadre (UIC) for useful comments. All computational chemistry calculations were done with the CHEMLAB-II molecular modeling package. M. Wiese, M. Piper, G. Krüger, K. R. Noll, and J. Keck are acknowledged for making some of the inhibition measurements reported in Table I that are not yet published.

Registry No. 1, 34332-19-9; **2**, 107114-72-7; **3**, 107114-73-8; **4**, 14571-23-4; **5**, 80-03-5; **6**, 107114-74-9; **7**, 35880-91-2; **8**, 107114-75-0; **9**, 80-08-0; **10**, 35880-83-2; **11**, 51688-26-7; **12**, 25963-47-7; **13**, 107114-76-1; **14**, 86552-09-2; **15**, 93427-46-4; **16**, 107114-77-2; **17**, 107114-78-3; **18**, 107114-79-4; **19**, 51688-31-4; **20**, 101513-28-4; **21**, 35881-03-9; **22**, 27147-69-9; **23**, 3572-34-7; **24**, 107114-80-7; **25**, 107114-81-8; **26**, 46948-43-0; **27**, 107114-82-9; **28**, 565-20-8; **29**, 17078-72-7; **30**, 4094-38-6; **31**, 107134-58-7; **32**, 34037-45-1; **33**, 7019-01-4; **34**, 86552-10-5; **35**, 7146-68-1; **36**, 1948-92-1; dihydropteroate synthase, 9055-61-2.

Synthesis and Antimalarial Effects of 4-[(7-Chloro-4-quinolinyl)amino]-2-[(diethylamino)methyl]-6-alkylphenols and Their N^{ω}-Oxides[1,2]

Stephen J. Kesten, Judith Johnson, and Leslie M. Werbel*

Warner-Lambert/Parke-Davis Pharmaceutical Research, Ann Arbor, Michigan 48105. *Received April 17, 1986*

A series of 4-[(7-chloro-4-quinolinyl)amino]-2-[(diethylamino)methyl]-6-alkylphenols and their N^{ω}-oxides were synthesized by the condensation of 4,7-dichloroquinoline and 4,7-dichloroquinoline N^{ω}-oxide with appropriately substituted 4-amino-2-[(diethylamino)methyl]-6-alkylphenol dihydrochlorides. The latter precursors were prepared in a six-step synthesis starting from available 2-alkylphenols. Several of the title compounds display potent antimalarial activity in mice.

Our recent report[1] of the potent antimalarial activity and unique properties of tebuquine (**1**) and related 5-[(7-chloro-4-quinolinyl)amino]-3-[(alkylamino)methyl][1,1′-biphenyl]-2-ols and N^{ω}-oxides stimulated a wider exploration of the effects of structural modification on antimalarial activity. Of particular concern was the nature of the requirement for a biphenylol system. We now report, therefore, the synthesis and biological activity of a series of 4-[(7-chloro-4-quinolinyl)amino]-2-[(diethylamino)-methyl]-6-alkylphenols and their N^{ω}-oxides (**2a–o**) as well as several closely related analogues.

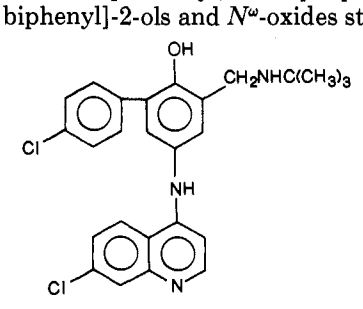

1

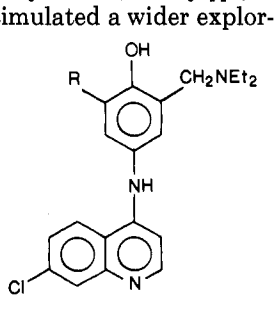

2

Chemistry. The synthetic scheme for the preparation of 4-[(7-chloro-4-quinolinyl)amino]-2-[(diethylamino)-methyl]-6-alkylphenols is outlined in Scheme I. The readily available appropriate 2-alkylphenols were treated with sodium nitrite and hydrochloric acid[3] to afford the corresponding 2-alkyl-2,5-cyclohexadiene-1,4-dione 4-oximes (**4**) in 22–65% yield (Table I). These were reduced catalytically with Raney nickel under ~50 psi of hydrogen, or in one case with sodium dithionite, and immediately acetylated with acetic anhydride to generate the corresponding N-(3-alkyl-4-hydroxyphenyl)acetamides (**5**) in 30–95% overall yields (Table II). These compounds were then treated with aqueous formaldehyde and diethylamine to provide the N-[5-[(diethylamino)methyl]-3-alkyl-4-hydroxyphenyl]acetamides (**6**) in 23–87% yields (Table III). Acidic hydrolysis gave the corresponding 4-amino-

(1) This is paper 61 of a series on antimalarial drugs. For paper 60, see: Werbel, L. M.; Cook, P. D.; Elslager, E. F.; Hung, J. H.; Johnson, J. L.; Kesten, S. J.; McNamara, D. J.; Ortwine, D. F.; Worth, D. F. *J. Med. Chem.* **1986**, *29*, 924.

(2) This investigation was supported by U.S. Army Medical Research and Development Command Contract DADA17-72-C-2077. This is contribution No. 1788 to the Army Research Program in Parasitic Diseases.

(3) Norris, R. K.; Sternhill, S. *Aust. J. Chem.* **1966**, *19*, 617.

0022-2623/87/1830-0906$01.50/0